

Article

QTL Mapping for Agronomic Important Traits in Well-Adapted Wheat Cultivars

Jingxian Liu ^{1,†}, Danfeng Wang ^{1,2,†} , Mingyu Liu ^{1,†}, Meijin Jin ¹, Xuecheng Sun ¹, Yunlong Pang ¹, Qiang Yan ¹, Cunzhen Liu ³ and Shubing Liu ^{1,*}

- ¹ National Key Laboratory of Wheat Improvement, College of Agronomy, Shandong Agricultural University, Taian 271018, China; a15562687757@163.com (J.L.); wdf19911025@live.com (D.W.); mingyuliu0531@163.com (M.L.); fpxwnbjmj@163.com (M.J.); xc12345687@126.com (X.S.); y.pang@sdau.edu.cn (Y.P.); 2022010006@sdau.edu.cn (Q.Y.)
- ² Key Laboratory of Plant Genetics and Molecular Breeding, Henan Key Laboratory of Crop Molecular Breeding & Bioreactor, Zhoukou Normal University, Zhoukou 466001, China
- ³ Tengzhou Bureau of Agriculture and Rural Affairs, Tengzhou 277500, China; lcu71@163.com
- * Correspondence: sbliu@sdau.edu.cn
- † These authors contributed equally to this work.

Abstract: Wheat (*Triticum aestivum* L.) is one of the most important food crops worldwide and provides the staple food for 40% of the world's population. Increasing wheat production has become an important goal to ensure global food security. The grain yield of wheat is a complex trait that is usually influenced by multiple agronomically important traits. Thus, the genetic dissection and discovery of quantitative trait loci (QTL) of wheat-yield-related traits are very important to develop high-yield cultivars to improve wheat production. To analyze the genetic basis and discover genes controlling important agronomic traits in wheat, a recombinant inbred lines (RILs) population consisting of 180 RILs derived from a cross between Xinong822 (XN822) and Yannong999 (YN999), two well-adapted cultivars, was used to map QTL for plant height (PH), spike number per spike (SNS), spike length (SL), grain number per spike (GNS), spike number per plant (SN), 1000-grain weight (TGW), grain length (GL), grain width (GW), length/width of grain (GL/GW), perimeter of grain (Peri), and surface area of grains (Sur) in three environments. A total of 64 QTL were detected and distributed on all wheat chromosomes except 3A and 5A. The identified QTL individually explained 2.24–38.24% of the phenotypic variation, with LOD scores ranging from 2.5 to 29. Nine of these QTL were detected in multiple environments, and seven QTL were associated with more than one trait. Additionally, Kompetitive Allele Specific PCR (KASP) assays for five major QTL *QSn-1A.2* (PVE = 6.82), *QPh-2D.1* (PVE = 37.81), *QSl-2D* (PVE = 38.24), *QTgw-4B* (PVE = 8.78), and *QGns-4D* (PVE = 13.54) were developed and validated in the population. The identified QTL and linked markers are highly valuable in improving wheat yield through marker-assisted breeding, and the large-effect QTL can be fine-mapped for further QTL cloning of yield-related traits in wheat.

Keywords: single nucleotide polymorphism; agronomic trait; linkage mapping; marker-assisted selection; Kompetitive Allele Specific PCR



Citation: Liu, J.; Wang, D.; Liu, M.; Jin, M.; Sun, X.; Pang, Y.; Yan, Q.; Liu, C.; Liu, S. QTL Mapping for Agronomic Important Traits in Well-Adapted Wheat Cultivars. *Agronomy* **2024**, *14*, 940. <https://doi.org/10.3390/agronomy14050940>

Academic Editor: Ainong Shi

Received: 2 April 2024

Revised: 24 April 2024

Accepted: 26 April 2024

Published: 30 April 2024



Copyright: © 2024 by the authors. Licensee MDPI, Basel, Switzerland. This article is an open access article distributed under the terms and conditions of the Creative Commons Attribution (CC BY) license (<https://creativecommons.org/licenses/by/4.0/>).

1. Introduction

Wheat (*Triticum aestivum* L.) is one of the most important food crops worldwide and provides the staple food for 40% of the world's population [1] with about 720 million tons being produced annually [2]. However, food shortages are becoming a serious problem with the rapid increase in the world's population and decrease in farmland. Thus, increasing wheat production is crucial to safeguarding global food security. The grain yield of wheat is a complex trait that is usually influenced by multiple agronomic important traits including plant height (PH), spike number per spike (SNS), spike length (SL), grain number per spike (GNS), spike number per plant (SN), 1000-grain weight (TGW),

etc., which are quantitatively controlled by multiple genes and are easily influenced by environments [3]. Thus, the genetic dissection and mining of quantitative trait loci (QTL) of wheat-yield-related traits are very important for developing high-yield cultivars to continuously improve wheat production.

With a size of about 17 Gb, wheat has a very large and complex genome. However, with the development of DNA sequencing technology, single nucleotide polymorphism (SNP) has been widely used as a marker in QTL mapping and genome-wide association studies (GWAS) due to the advantages of abundance of SNPs in the wheat genome. The advantages of SNP markers include the fact that the genotyping error rates tend to be lower [4,5], and larger numbers of markers can be run jointly, while genotype determination is completely automatic, eliminating what is generally the most important cost element of genotyping [4,6]. In recent years, the development of wheat 90K, 55K, and 660K SNP arrays has dramatically accelerated the study of wheat genetic diversity and QTL mapping [7–10]. The 55K wheat SNP array consists of 53,063 tags and has been widely used in recent studies due to its advantages such as genome specificity, higher polymorphism, informativeness, cost-effectiveness, etc. [10–12].

QTL are beneficial gene resources for molecular breeding in wheat improvement, which are useful for marker-assisted selection (MAS). In recent years, many QTL controlling agronomic traits have been mapped in wheat. QTL associated with PH have been identified on almost all 21 chromosomes [3,13]. Stable and major QTL controlling grain shape and size have been mapped on chromosomes 2A, 2D, 4A, 5A, 5B, and 6A [14–16]. Stable QTL for SL have been mapped on chromosomes 1A, 1B, 2D, 3A, 3B, 4A, 4B, 5A, 5B, 6A, 6B, 6D, 7A, 7B, and 7D in many studies [3,7–21]. QTL explaining over 10% of the phenotypic variation for TGW have been identified on chromosomes 1A, 1B, 2D, 3A, 3D, 4A, 4B, 5A, 5B, 5D, 6A, 6D, 7A, and 7D [22–25].

Although a large number of QTL for important agronomic traits have been identified, most studies of QTL mapping for agronomic traits usually used populations derived from crosses between landraces, or ancient cultivars with distinct phenotypes differences, and the favorable QTL mapped in landrace or ancient varieties cannot be used directly as parents to make crosses in breeding due to their poor agronomic trait performance, which greatly restricts the potential use of the QTL in breeding. To cope with this problem, using well-adapted high-yield cultivars as parents to develop populations to map QTL for agronomically important traits has more advantages to use the mapped favorable QTL in breeding, because the well-adapted cultivars have elite agronomic trait performance, and can be used as parents to make crosses directly to further improve the yield potential of modern varieties through MAS.

In the present study, a recombinant inbred line (RIL) population was developed from a cross between the two elite wheat cultivars Yannong 999 (YN999) and Xinong 822 (XN822). The population was measured for agronomic traits under multiple environments (years) and genotyped by 55K SNP array. The objectives were to: (1) Construct a high-density genetic map to map QTL controlling important agronomic traits in widely planted elite wheat cultivars in wheat production; (2) identify novel major QTL in elite wheat cultivars and develop Kompetitive Allele Specific PCR (KASP) markers closely linked with those QTL for MAS and further fine-mapping. Our results will lay a solid foundation for further yield improvement of modern wheat varieties through MAS breeding.

2. Materials and Methods

2.1. Plant Materials

The plant materials used in this study include YN999, XN822, and 180 RILs developed from the cross between XN822 and YN999 by single seed descent. YN999 is a semi-winter, more spike-type wheat cultivar, with the advantages of longer spikes, more grains, wide adaptability, and strong cold tolerance. It is one of the major varieties widely used in wheat production in the Yellow and Huaihe River wheat region. XN822 is a semi-winter, early

maturing cultivar, which has a thicker stalk, a semi-compact plant type, higher tillering ability, and high grain weight.

2.2. Evaluation of Agronomic Traits

The RILs and the two parents were planted in the field experiments with two replicates using randomized complete blocks design (RCBD) at the Experimental Station of Shandong Agriculture University in Taian (Longitude: 117.155985; Latitude: 36.164572; Altitude: 125 m) during the 2020–2021 and 2021–2022 wheat-growing seasons and in Zhoukou (Longitude: 114.68304; Latitude: 33.635975; Altitude: 49 m), Henan province, during the 2021–2022 wheat-growing season. In each experiment, seeds of each line were space planted 6 cm apart in a 3.0 m long single-row plot with 25 cm between rows. Standard cultivation practice was followed in all field experiments. PH, SNS, SL, GNS, and SN were investigated according to the methods described by Sun et al. [26]. After harvesting, the seeds were air-dried, and then the grain-related traits, including TGW, grain length (GL), grain width (GW), length/width of grain (GL/GW), perimeter of grain (Peri), and surface area of grains (Sur) were scanned by a WSEN SC-G automated seed assay analyzer (Wanshen Testing Technology Co., Ltd., Hangzhou, China) [8].

2.3. Statistical Analysis

Descriptive statistics and Pearson correlation analysis were calculated using SPSS V27 software [27]. The correlation plot was constructed using Origin 2022b (Origin Lab Corporation, Northampton, MA, USA) software. The phenotypic means were calculated using the “AVERAGE” function, and a Student’s *t* test was analyzed using the T-test function implemented in Excel 2016 software. Analysis of variance was conducted using general linear modeling (GLM) and multiple comparison was analyzed using a Duncan test by SPSS V27 software. Heritability was calculated according to the following formula:

$$H = Vg / (Vg + Vge/L + Ve/RL)$$

where *Vg* is the genetic variance; *Vge* is the genetic and environmental interaction variance, *Ve* is the residual variance, *R* is the number of replicates, and *L* is the number of environments.

2.4. SNP Genotyping

Genomic DNA, including RILs and the two parents, was extracted from fresh leaves using a modified CTAB method [28]. The quality of all DNA samples was screened on 1% agarose gels for quality control and then genotyped using the Wheat 55K SNP array containing 53,063 SNP markers by CapitalBio Technology (Beijing, China). Chip genotyping was based on the Axiom[®] 2.0 Assay for 384 Samples User Guide [10].

2.5. Linkage Analysis and QTL Mapping

After genotyping with the Wheat55K SNP array, SNPs that showed polymorphism between YN999 and XN822 were picked out. Then, those polymorphic SNPs with a missing proportion of more than 1% or a heterozygous proportion of more than 10% were excluded. The eligible SNPs were binned based on their segregation patterns [29] using the BIN function of IciMapping V4.1 (<https://isbreedingen.caas.cn/software/qtlcimapping/294606.htm>, (accessed on 12 May 2023)). Genetic linkage maps were generated using IciMapping V4.1 software. A Kosambi mapping function was used to convert recombination fractions into map distances. QTL mapping was conducted in IciMapping V4.1 software in the biparental populations (BIP) module with inclusive composite interval mapping (ICIM). The walking speed for all QTL was 1.0 cM. A LOD score of 2.5 was set as a threshold for declaring the presence of a QTL [8].

2.6. Marker Development and QTL Validation in RIL Population

For some QTL detected in more than one environment with large genetic effects, one SNP located in each of the QTL intervals was converted into KASP markers and run across the RIL population to further validate the effectiveness and accuracy of KASP markers as well as the genetic effects of each QTL.

For KASP marker screening, the PCR amplification was performed in a T960 Touch cycler (Heal Force, Shanghai, China) with the following PCR cycling parameters: hot start at 94 °C for 15 min, followed by 10 touchdown cycles (94 °C for 20 s; touchdown at 65 °C initially and decreasing by −0.8 °C per cycle for 25 s), followed by 30 additional cycles of denaturation and annealing/extension (94 °C for 10 s; 57 °C for 60s). The KASP assays were visualized in a Fluostar Omega microplate reader (BMG Labtech, Ortenberg, Germany) and analyzed using Klustercaller software (Version = 4.1.2.26268, LGC group, Teddington, UK) [30].

3. Results

3.1. Phenotypic Variation

The PH, GNS, SN, TGW, GL, GW, Sur, and Peri of XN822 were higher than that of YN999. The SL, SNS, and GL/GW of YN999 were higher than that of XN822 (Figure 1, Table 1); the apparent difference of the 11 traits between the two parents indicated that they were suitable parental lines for the population. Among the RILs, all measured traits showed high variability in all environments, and significant differences between environments were observed for most of the traits. The continuous distribution of phenotypes suggested that multiple QTL may be involved in controlling those traits in the population (Figure 1). Transgressive segregation was observed in all experiments for all traits, suggesting that favorable allele governing the traits may originate from both parents. In addition, broad-sense heritability (H^2) ranged from 48.6 to 89.0% for the 11 traits. The H^2 for PH, GNS, and GL was higher than 80%, while it was lower than 60% for SNS, SN, GW, and Sur.

Table 1. Summary of the agronomic traits in the ‘XN822 × YN999’ RIL population.

Traits	Env.	Parents		RIL					
		XN822	YN999	Min	Max	Mean	SD	CV (%)	Heritability (%)
PH	2020TA	87.26	83.59	63.13	107.50	84.10 a	7.19	8.55	89.0
	2021TA	60.50	59.25	48.00	85.00	64.29 c	5.13	7.97	
	2021ZK	83.90	77.10	57.50	94.88	78.56 b	6.33	8.06	
SL	2020TA	10.26	11.16	8.00	14.44	10.76 a	1.07	9.98	72.2
	2021TA	8.06	8.76	6.38	10.38	8.42 b	0.83	9.85	
	2021ZK	8.36	7.78	5.90	11.68	8.53 b	1.09	12.78	
GNS	2020TA	70.56	65.21	53.38	104.20	69.68 a	8.18	11.74	80.3
	2021TA	53.63	55.88	39.25	79.13	58.61 b	6.34	10.82	
	2021ZK	58.43	49.72	24.80	59.60	47.01 c	8.57	18.23	
SNS	2020TA	20.596	22.34	19.25	24.80	22.23 a	0.94	4.25	49.4
	2021TA	17.13	18.88	17.13	20.88	18.94 b	0.83	4.37	
	2021ZK	19.56	18.33	14.20	22.20	18.91 b	1.52	8.03	
SN	2020TA	8.41	8.56	6.88	16.00	10.90 a	1.61	14.82	48.6
	2021TA	4.13	4.25	3.13	7.63	4.99 c	0.63	12.65	
	2021ZK	6.76	5.33	2.60	17.20	8.15 b	2.67	32.76	
TGW	2020TA	52.65	46.78	25.22	61.07	47.40 a	6.66	14.05	61.6
	2021TA	53.61	49.56	35.85	60.31	49.54 a	4.90	9.88	
GL	2020TA	5.54	5.27	4.97	6.63	5.66 b	0.30	5.23	84.6
	2021TA	6.32	6.12	5.65	7.60	6.61 a	0.33	5.01	
GW	2020TA	3.05	2.61	2.29	3.27	2.82 b	0.21	7.35	48.8
	2021TA	3.45	3.24	2.97	3.70	3.36 a	0.15	4.36	

Table 1. Cont.

Traits	Env.	Parents					RIL			
		XN822	YN999	Min	Max	Mean	SD	CV (%)	Heritability (%)	
GL/GW	2020TA	1.96	2.13	1.70	2.45	2.02 a	0.14	7.05	73.9	
	2021TA	1.85	2.00	1.70	2.39	1.98 a	0.11	5.51		
Sur	2020TA	12.35	11.45	9.46	16.03	12.67 b	1.37	10.85	59.2	
	2021TA	17.11	16.12	13.63	21.50	17.54 a	1.38	7.84		
Peri	2020TA	15.37	14.23	12.77	16.10	14.31 b	0.71	4.97	72.5	
	2021TA	17.25	15.72	14.58	18.87	16.86 a	0.74	4.36		

PH, plant height (cm); SNS, spikelet number per spike; SL, spike length (cm); GNS, kernel number per spike; SN, spike number per plant; TGW, 1000-grain weight (g); GL, grain length (mm); GW, grain width (mm); GL/GW, length/width of grain; Peri, perimeter of grain (mm); Sur, surface area of grains per plant (mm²); RIL, recombinant inbred lines; Min, minimum value; Max, maximum value; Mean, the sum of the data divided by the number of data; SD, standard deviation; CV, coefficient of variation; H², the broad-sense heritability; 2020TA, in Taian during the 2020–2021 wheat-growing season; 2021TA, in Taian during the 2021–2022 wheat-growing season; 2021ZK, in Zhoukou during the 2021–2022 wheat-growing season. Lowercase letters beside the mean indicate multiple comparison (Duncan test) among environments for each trait at the significant level of $p < 0.05$.

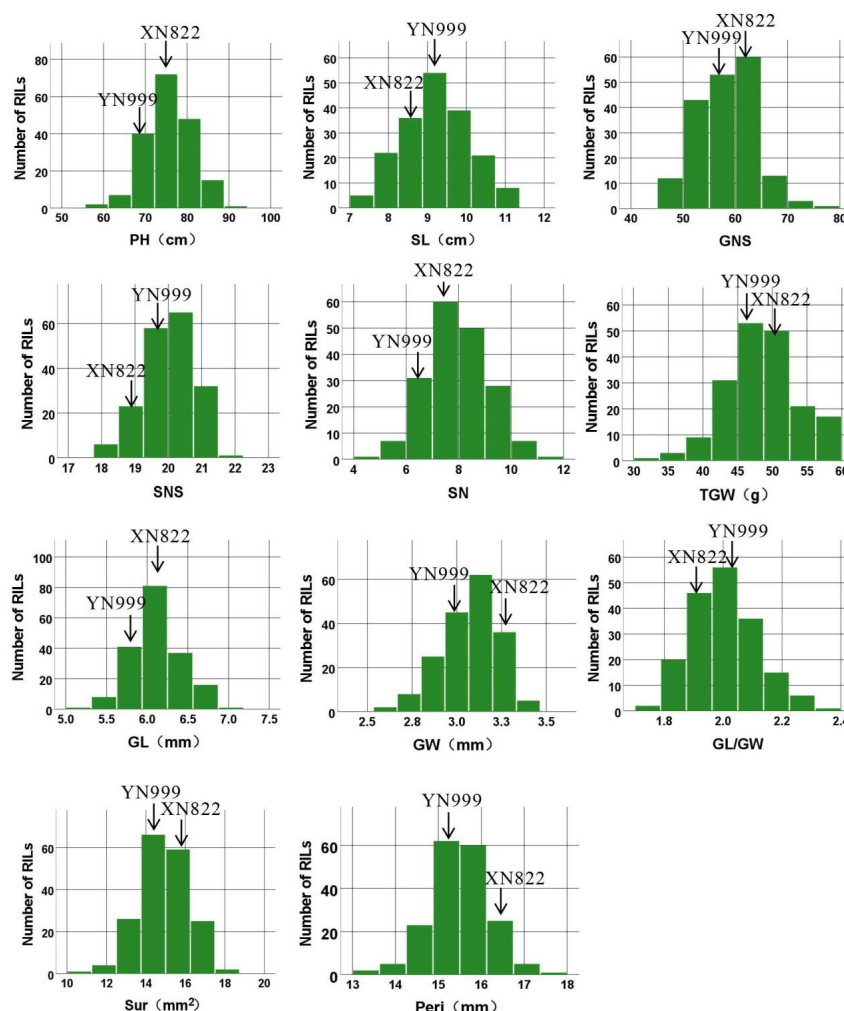


Figure 1. Phenotypic distribution of agronomic traits in ‘XN822 × YN999’ RIL population. PH, plant height (cm); SNS, spikelet number per spike; SL, spike length (cm); GNS, kernel number per spike; SN, spike number per plant; TGW, 1000-grain weight (g); GL, grain length (mm); GW, grain width (mm); GL/GW, length/width of grain; Peri, perimeter of grain (mm); Sur, surface area of grains per plant (mm²); RILs, recombinant inbred lines; X-axis is the value of the phenotypes and Y-axis is the number of RILs.

The correlation for agronomic traits analyzed using the average values across three environments showed that GL/GW was negatively correlated with PH, SL, SNS, GNS, GW, and TGW, whereas TGW was negatively correlated with GNS. Positive correlations among PH, SL, SNS, SN, GNS, GL, GW, Sur, and Peri were observed (Figure 2).

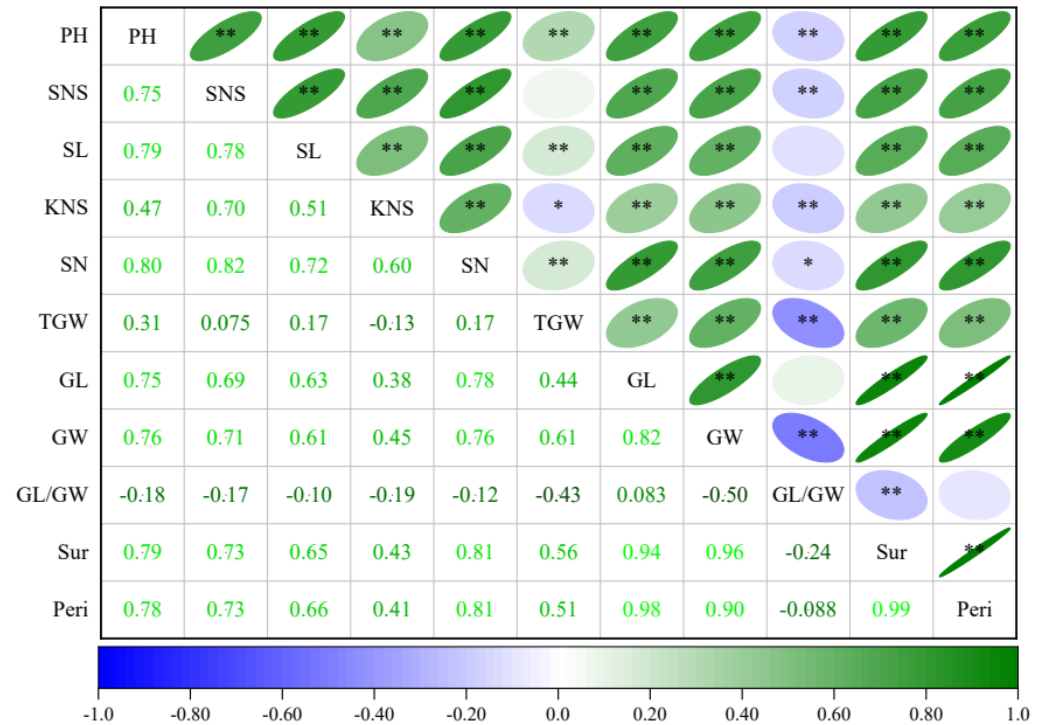


Figure 2. Correlation analysis of the mean values of traits collected from three environments. PH, plant height (cm); SNS, spikelet number per spike; SL, spike length (cm); GNS, kernel number per spike; SN, spike number per plant; TGW, 1000-grain weight (g); GL, grain length (mm); GW, grain width (mm); GL/GW, length/width of grain; Peri, perimeter of grain (mm); Sur, surface area of grains per plant (mm²). The upper triangular illustrates the correlations using areas and colors of ellipses. Right and left oblique ellipses indicate positive and negative correlations, respectively. * and ** refer to the significance at the level of 0.05 and 0.01. The ellipses without * refer to no significance. The lower triangular lists the values of correlation coefficients (r) with different colors.

3.2. Genetic Linkage Map Construction

After genotyping the RILs and the two parents, 17,902 SNPs (33.7% of the total SNPs) detected polymorphism between YN999 and XN822 and were used to construct the linkage map. A genetic linkage map covering 3026.07 cM was constructed with 12,141 SNP markers distributed on 21 chromosomes (Table 2). The chromosomes' length ranged from 65.59 cM (chromosome 4D) to 331.58 cM (chromosome 2D). For the three sub-genomes, A genome contained the most SNP markers (4675), with a total genetic distance of 855.76 cM; B genome contained 4516 SNP markers, with a total genetic distance of 853.71 cM; D genome contained the fewest SNP markers (2950), while showing the longest total genetic distance (1316.6 cM).

Table 2. The genetic linkage map constructed by the ‘Xinong822 × Yannong999’ RIL population.

Chromosome	Number of SNP Markers	Length (cM)	Max Interval (cM)
1A	883	93.47	10.66
1B	383	88.71	18.86
1D	743	229.05	36.79
2A	552	165.63	37.29
2B	747	160.04	62.12
2D	905	331.58	52.76
3A	527	152.47	15.47
3B	861	170.13	36.06
3D	103	118.09	15.87
4A	665	99.06	10.88
4B	425	98.23	9.97
4D	163	65.59	13.95
5A	875	75.54	7.6
5B	436	116.16	25.01
5D	503	205.56	13.96
6A	458	148.31	43.63
6B	501	97.61	8.54
6D	176	102.98	31.58
7A	715	121.28	10.5
7B	1163	122.83	20.92
7D	357	263.75	51.2
A genome	4675	855.76	43.63
B genome	4516	853.71	62.12
D genome	2950	1316.6	52.76
Whole genome	12141	3026.07	62.12

Number of SNP markers: SNP number mapped in the linkage map; Length: length of linkage map; Max interval: maximum genetic distance between two adjacent SNP markers.

3.3. QTL Analysis

In total, 64 QTL distributed on 19 chromosomes except for 3A and 5A for the 11 traits were identified with the explained phenotypic variation (PVE) ranging from 2.24 to 38.24%, and the LOD scores ranging from 2.54 to 29. Nine of these QTL were detected in multiple environments (Table 3).

Table 3. QTL for evaluated agronomic traits in the ‘XN822 × YN999’ RIL population.

Traits	QTL	Environment	Chromosome	Position (cM)	Left Marker	Right Marker	LOD	PVE (%)	Add
PH	<i>QPh-1A</i>	2020TA	1A	49.44–64.54	AX-111149806	AX-111456614	4.00	4.31	1.50
	<i>QPh-2B</i>	2021TA	2B	74.97–75.26	AX-111667781	AX-109974562	3.67	3.16	0.92
	<i>QPh-2D.1</i>	2020TA	2D	54.33–68.32	AX-109403444	AX-110836537	21.33	28.88	3.89
		2021TA	2D	53.47–57.06	AX-108988107	AX-110647062	29.40	37.81	3.18
		2021ZK	2D	54.33–68.32	AX-109403444	AX-110836537	11.34	21.32	2.94
	<i>QPh-2D.2</i>	2021TA	2D	110.54–111.72	AX-111780198	AX-110515536	3.88	3.36	−0.96
	<i>QPh-3B.1</i>	2021ZK	3B	14–14.29	AX-111011119	AX-109478402	4.20	6.97	−1.69
	<i>QPh-3B.2</i>	2021TA	3B	34.07–35.59	AX-109915590	AX-110956452	2.54	2.24	−0.77
	<i>QPh-4A</i>	2021TA	4A	64.25–67.82	AX-109305727	AX-111032494	6.20	5.54	−1.21
	<i>QPh-6B</i>	2020TA	6B	16.57–17.15	AX-108823992	AX-109458406	6.46	7.15	−1.95
	<i>QPh-6D</i>	2021TA	6D	56.9–60.54	AX-109847629	AX-109346183	6.75	6.26	−1.30
	<i>QPh-7A</i>	2020TA	7A	64.8–68.08	AX-109420524	AX-108857319	3.68	3.88	−1.42
	<i>QPh-7D.1</i>	2021TA	7D	142.56–150.32	AX-108999245	AX-89703036	2.99	3.10	−0.90
		2021ZK	7D	151.77–152.37	AX-94571320	AX-109561428	3.28	5.36	−1.46
		2020TA	7D	254.98–255.27	AX-110271452	AX-109112266	9.48	10.76	2.37
<i>QPh-7D.2</i>	2021TA	7D	254.98–255.27	AX-110271452	AX-109112266	10.32	9.73	1.61	
	2021ZK	7D	254.98–255.27	AX-110271452	AX-109112266	5.49	9.18	1.93	
	SL	<i>QSI-2A</i>	2020TA	2A	9.77–2.52	AX-110685697	AX-110907781	2.61	3.03
2021TA			2A	9.77–2.52	AX-110685697	AX-110907781	6.73	7.66	0.23
2021ZK			2A	9.77–2.52	AX-110685697	AX-110907781	4.38	10.98	0.36
<i>QSI-2D</i>		2020TA	2D	54.33–68.32	AX-109403444	AX-110836537	25.44	38.24	0.67
		2021TA	2D	54.33–68.32	AX-109403444	AX-110836537	24.01	33.25	0.48
SL	<i>QSI-3D</i>	2021ZK	3D	18.68–33.57	AX-89666287	AX-111183309	3.01	7.69	−0.30
	<i>QSI-4A</i>	2020TA	4A	27.47–32.16	AX-109017673	AX-109278499	7.80	9.49	−0.33
	<i>QSI-4B</i>	2021TA	4B	52.14–60.74	AX-109376424	AX-110445790	5.28	5.59	−0.20
	<i>QSI-5D</i>	2020TA	5D	156.91–164.41	AX-111008575	AX-109820798	6.80	8.64	−0.32
	<i>QSI-6D</i>	2021TA	6D	90.63–102.98	AX-109532654	AX-109471603	3.33	3.95	0.17
	<i>QSI-7B</i>	2020TA	7B	5.86–11.22	AX-94902381	AX-112287959	4.70	5.34	−0.25
	<i>QSI-7D</i>	2020TA	7D	161.04–214.66	AX-111479908	AX-111077348	3.48	7.99	−0.30

Table 3. Cont.

Traits	QTL	Environment	Chromosome	Position (cM)	Left Marker	Right Marker	LOD	PVE (%)	Add
SNS	<i>QSns-1A.1</i>	2021TA	1A	25–28.11	AX-108957758	AX-110050825	5.46	10.00	−0.26
	<i>QSns-1A.2</i>	2020TA	1A	91.4–92.89	AX-111799412	AX-109109679	3.84	6.82	0.25
		2021TA	1A	91.4–92.89	AX-111799412	AX-109109679	2.59	4.59	0.18
	<i>QSns-1B</i>	2021TA	1B	77.6–79.3	AX-108942270	AX-108964977	3.36	5.89	−0.20
	<i>QSns-2B</i>	2020TA	2B	123.15–126.3	AX-111069661	AX-109980364	3.32	5.96	−0.23
	<i>QSns-2D.1</i>	2021TA	2D	86.4–91.46	AX-109382452	AX-111593514	4.51	8.15	0.24
	<i>QSns-2D.2</i>	2020TA	2D	240.23–254.85	AX-109361861	AX-94502054	3.41	6.10	−0.23
	<i>QSns-6A.1</i>	2020TA	6A	91.82–93.72	AX-110365398	AX-109896154	2.76	4.81	−0.21
<i>QSns-6A.2</i>	2021TA	6A	98.32–100.44	AX-109321632	AX-109910549	4.45	8.35	−0.24	
GNS	<i>QGns-2A.1</i>	2020TA	2A	10.07–12.15	AX-110530257	AX-111018125	3.22	5.79	1.98
	<i>QGns-2A.2</i>	2020TA	2A	50.27–51.84	AX-111651930	AX-111017366	6.43	12.05	−2.85
	<i>QGns-3B</i>	2021TA	3B	158.59–169.54	AX-111145295	AX-109391294	5.05	8.83	−1.93
	<i>QGns-4A</i>	2020TA	4A	88.73–91.78	AX-111648542	AX-110550799	3.16	4.65	1.76
		2021TA	4A	83.29–88.44	AX-110540586	AX-109987309	10.31	18.24	2.71
	<i>QGns-4D</i>	2020TA	4D	56.89–65.59	AX-111024002	AX-89578133	6.93	13.54	−3.02
		2021TA	4D	56.89–65.59	AX-111024002	AX-111241478	6.61	12.16	−2.22
<i>QGns-6A</i>	2021ZK	6A	94.3–96.77	AX-110423063	AX-109333111	3.02	7.40	−2.33	
SN	<i>QSn-1B</i>	2021ZK	1B	72.24–75.09	AX-109384977	AX-109836324	2.64	6.68	0.69
	<i>QSn-6A</i>	2020TA	6A	3.4–11.81	AX-109915394	AX-111011118	3.06	7.78	0.45
TGW	<i>QTgw-1D</i>	2021TA	1D	110.93–114.31	AX-109816030	AX-109146253	3.76	5.26	1.13
	<i>QTgw-2A</i>	2021TA	2A	54.66–58.16	AX-111581446	AX-109303703	4.44	6.50	1.26
	<i>QTgw-4A</i>	2021TA	4A	78.16–79.15	AX-110440161	AX-109924488	10.44	16.21	−1.98
	<i>QTgw-4B</i>	2021TA	4B	42.22–44.34	AX-109931786	AX-108813019	5.93	8.43	−1.45
		2020TA	4B	43.38–45.22	AX-110973841	AX-110436318	4.05	8.78	−1.99
<i>QTgw-7B</i>	2021TA	7B	108.2–115.5	AX-110676189	AX-109902211	3.27	5.91	1.20	
GL	<i>QGl-2A</i>	2021TA	2A	54.36–54.66	AX-108822367	AX-111576466	9.51	14.53	0.13
	<i>QGl-4A.1</i>	2021TA	4A	34.61–35.65	AX-109882402	AX-108892678	7.55	11.09	−0.11
	<i>QGl-4A.2</i>	2020TA	4A	79.73–83.01	AX-111592727	AX-109363749	4.96	10.19	−0.10
	<i>QGl-6A</i>	2021TA	6A	134.15–134.76	AX-111680204	AX-110433692	3.73	5.20	0.08
	<i>QGl-6D</i>	2021TA	6D	90.63–102.98	AX-109532654	AX-109471603	3.15	4.22	−0.07
	<i>QGl-7A</i>	2021TA	7A	37.59–38.19	AX-109334017	AX-110536946	2.90	3.96	0.07
	<i>QGl-7B</i>	2020TA	7B	42.57–45.17	AX-111044151	AX-89749267	2.89	5.72	0.07

Table 3. Cont.

Traits	QTL	Environment	Chromosome	Position (cM)	Left Marker	Right Marker	LOD	PVE (%)	Add
GW	<i>QGw-2D</i>	2020TA	2D	292.51–292.86	AX-108791923	AX-109444904	3.00	6.92	−0.05
	<i>QGw-4B</i>	2021TA	4B	36.03–37.18	AX-111620391	AX-109909153	2.72	6.14	−0.04
Peri	<i>QPeri-1A</i>	2021TA	1A	30.16–31.09	AX-110527733	AX-109986286	3.71	3.91	0.15
	<i>QPeri-2A</i>	2021TA	2A	54.36–54.66	AX-108822367	AX-111576466	6.76	7.15	0.20
	<i>QPeri-2B.1</i>	2021TA	2B	0–1.18	AX-111741075	AX-94488983	7.02	7.30	−0.20
	<i>QPeri-2B.2</i>	2021TA	2B	143.39–147.69	AX-111680931	AX-109477763	4.40	4.58	0.16
	<i>QPeri-3D</i>	2021TA	3D	47.79–49.89	AX-95634629	AX-110040152	11.84	14.06	0.28
	<i>QPeri-4A.1</i>	2021TA	4A	34.61–35.65	AX-109882402	AX-108892678	7.00	7.27	−0.20
	<i>QPeri-4A.2</i>	2020TA	4A	79.73–83.01	AX-111592727	AX-109363749	3.22	7.48	−0.20
Peri	<i>QPeri-5B</i>	2020TA	5B	13.61–14.78	AX-108913498	AX-110446007	2.59	6.27	0.18
	<i>QPeri-5D.1</i>	2021TA	5D	121.88–123.05	AX-109924594	AX-110035093	2.94	3.05	−0.13
	<i>QPeri-5D.2</i>	2021TA	5D	192.55–192.85	AX-111354812	AX-108991233	7.21	7.55	0.20
Sur	<i>QSur-1A</i>	2021TA	1A	30.16–31.09	AX-110527733	AX-109986286	4.25	8.90	0.41
	<i>QSur-2A</i>	2021TA	2A	54.36–54.66	AX-108822367	AX-111576466	3.72	7.48	0.38
	<i>QSur-5B</i>	2020TA	5B	13.61–14.78	AX-108913498	AX-110446007	3.15	7.10	0.37

Note: LOD, logarithm of odds; PVE, phenotypic variation explained; Add, additive effect; left marker and right marker indicate the left and right boundaries of the confidence interval. Positive additive effects indicate that the allele increasing its phenotypic value is from YN999, and negative additive effects indicate that the allele increasing its phenotypic value is from XN822. PH, plant height (cm); SNS, spikelet number per spike; SL, spike length (cm); GNS, grain number per spike; SN, spike number per plant; TGW, 1000-grain weight (g); GL, grain length (mm); GW, grain width (mm); GL/GW, length/width of grain; Peri, perimeter of grain (mm); Sur, surface area of grains per plant (mm²); 2020TA, in Taian during the 2020–2021 wheat-growing season; 2021TA, in Taian during the 2021–2022 wheat-growing season; 2021ZK, in Zhoukou during the 2021–2022 wheat-growing season.

3.3.1. PH and SN

A total of 12 QTL for PH were mapped on chromosomes 1A, 2B, 2D (2), 3B (2), 4A, 6B, 6D, 7A, and 7D (2), which explained 2.24–37.81% of the phenotypic variation. Among them, *QPh-2D.1* was detected in all three environments and explained 21.32%, 28.88%, and 37.81% of the phenotypic variation, respectively (Figure 3a). *QPh-7D.2* was also detected in all three environments and explained 9.18%, 9.73%, and 10.76% of the phenotypic variation, respectively. The positive alleles of *QPh-2D.1* and *QPh-7D.2* were from YN999. *QPh-7D.1* was detected in the 2021TA and 2021ZK experiments and explained 3.10% and 5.36% of the phenotypic variation, respectively. The positive allele of *QPh-7D.1* was from XN822 (Table 3). Only two QTL for SN were mapped on chromosomes 1B and 6A with an explained phenotypic variation of 6.68% and 7.78%, respectively (Table 3).

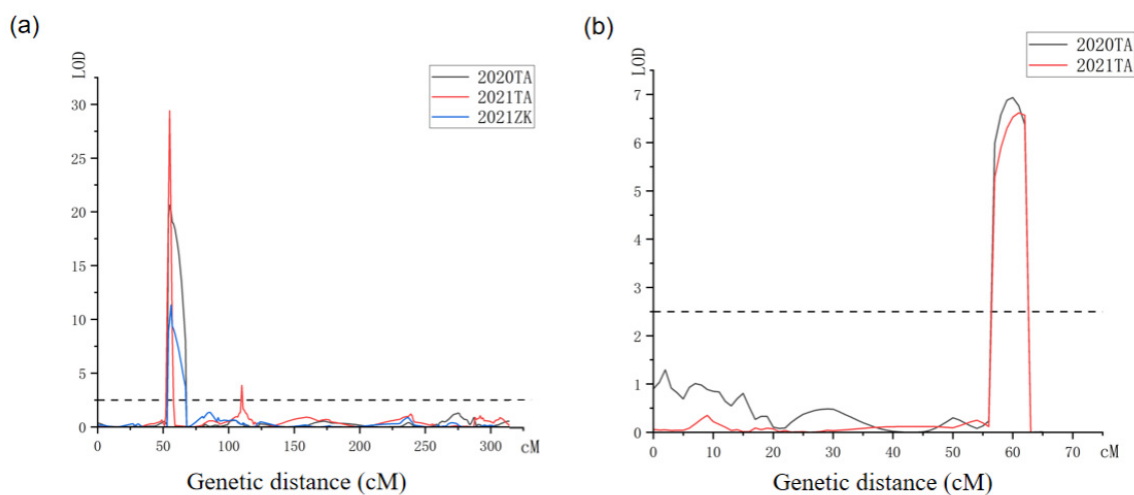


Figure 3. Major QTL *QPh-2D.1* (a) and *QGns-4D* (b) mapped in ‘XN822/YN999’ RILs population by inclusive composite interval mapping (ICIM) in multi-environments. Dotted line represents the logarithm of the odd (LOD) = 2.5.

3.3.2. Spike Traits

Nine QTL for SL were mapped on chromosomes 2A, 2D, 3D, 4A, 4B, 5D, 6D, 7B, and 7D, which explained 3.03–38.24% of the phenotypic variation. Among them, *QSl-2A* was detected in all three experiments and explained 3.03%, 7.66%, and 10.98% of the phenotypic variation, respectively. *QSl-2D* was detected in two experiments (2020TA and 2021TA) and explained 33.25% and 38.24% of the phenotypic variation, respectively. The positive alleles of the two QTL were all contributed to by YN999.

Eight QTL for SNS were mapped on chromosomes 1A (2), 1B, 2B, 2D (2), and 6A (2), which explained 4.59–10.00% of the phenotypic variation. Only *QSns-1A.2* was detected in two experiments (2020TA and 2021TA) and explained 4.59% and 6.82% of the phenotypic variation, respectively. The positive allele of this locus was contributed to by YN999.

Six QTL for GNS were mapped on chromosomes 2A (2), 3B, 4A, 4D, and 6A and explained 4.65–18.24% of the phenotypic variation. Two of them, *QGns-4A* and *QGns-4D*, were detected in the 2020TA and 2021TA experiments. *QGns-4A* explained 4.65% and 18.24% of the phenotypic variation, respectively. The positive allele of this locus was contributed to by YN999. *QGns-4D* explained 13.54% and 12.16% of the phenotypic variation, respectively, whereas the positive allele of this locus was contributed to by XN822 (Figure 3b).

3.3.3. Grain Traits

Five QTL for TGW were mapped on chromosomes 1D, 2A, 4A, 4B, and 7B, which explained 5.26–16.21% of the phenotypic variation. Among them, *QTgw-4B* was detected

in the 2021TA and 2020TA experiments and explained 8.43% and 8.78% of the phenotypic variation, respectively. The positive allele of this locus was contributed to by XN822.

Seven QTL for GL were mapped on chromosomes 2A, 4A (2), 6A, 6D, 7A, and 7B, which explained 3.96–14.53% of the phenotypic variation. All of them were detected only in one environment, with *QGl-2A* explaining the largest phenotypic variation (14.53%). Only two QTL for GW were mapped in one environment on chromosomes 4B and 2D.

A total of 10 QTL for Peri were mapped on chromosomes 1A, 2A, 2B (2), 3D, 4A (2), 5B, and 5D (2) and explained 3.05–14.06% of the phenotypic variation. All of them were identified only in one environment. Three QTL for Sur were mapped on chromosomes 1A, 2A, and 5B, and explained 7.10–8.90% of the phenotypic variation. All of them were identified only in one environment (Table 3).

3.4. Validation of the Major QTL in the RIL Population

Because *QSns-1A.2*, *QPh-2D.1*, *QSI-2D*, *QTgw-4B*, and *QGns-4D* were detected in multiple environments with large genetic effects, it is likely that these are stable QTL with major effects on SNS, PH, SL, TGW, and GNS, respectively. Four SNPs located in these QTL intervals were converted into KASP assays (Table 4) to screen the RIL population, and all of them separated the two genotypes at each locus clearly (Table 4, Figure 4).

Table 4. The developed primer sequences of KASP assays for five mapped QTL.

QTL	Probe ID	Mutation Site	Forward Primer Sequence (5'-3')	Reverse Primer Sequence (5'-3')
<i>QTgw-4B</i>	AX-110935921	T//G	GAAGGTGACCAAGTTCATGCTTGCA TGCTGGTGGTTACAG GAAGGTCGGAGTCAACGGATTGCA TGCTGGTGGTTACCAT	CGCCAGACACCATTAGCCTT
<i>QPh-2D.1/QSI-2D</i>	AX-110836537	T//C	GAAGGTGACCAAGTTCATGCTGCAT TTCCCATGGTTTTAGCTCT GAAGGTCGGAGTCAACGGATTGCAT TTCCCATGGTTTTAGCTCC	CCCCGGTCATGCAATCAAGA
<i>QSns-1A.2</i>	AX-111567464	T//C	GAAGGTGACCAAGTTCATGCTACCC TGCCTAAAATACTATTGTGC GAAGGTCGGAGTCAACGGATTACCC TGCCTAAAATACTATTGTGT	GCGGAGGAGAGGAAGAGGTA
<i>QGns-4D</i>	AX-111024002	A//C	GAAGGTGACCAAGTTCATGCTTGTA AGATGGAAGTCTGGGTA GAAGGTCGGAGTCAACGGATTGTA AGATGGAAGTCTGGGTC	GCACATGCGTTTGAGGTCAT

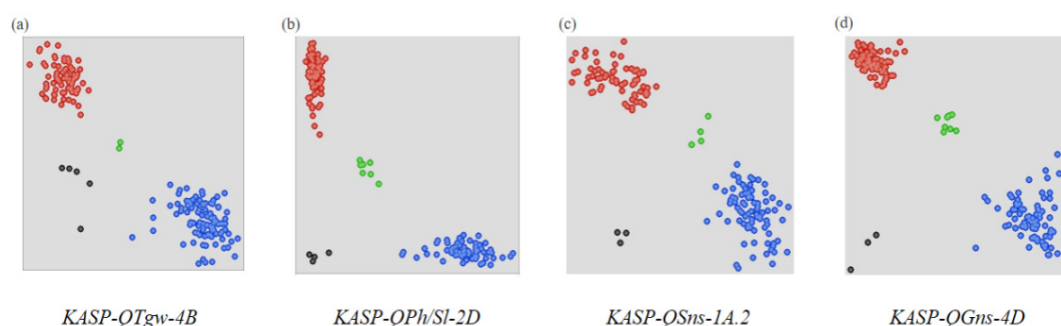


Figure 4. KASP assay of five QTL (*QTgw-4B* (a), *QPh-2D.1/QSI-2D* (b), *QSns-1A.2* (c) and *QGns-4D* (d)) in the RILs population. The red and blue dots represent the HEX and FAM labelled allele, respectively. The green dots represent heterozygotes and the black dots represent negative controls (ddH₂O).

QSns-1A.2 was detected in the 2020TA and 2021TA experiments; it is possible that this QTL is more stable than the other minor QTL for SNS in YN999. As expected, SNS of the RILs conferring the allele from YN999 significantly increased SNS by 1.39% and 1.56% in the 2020TA and 2021TA experiments, respectively (Figure 5a).

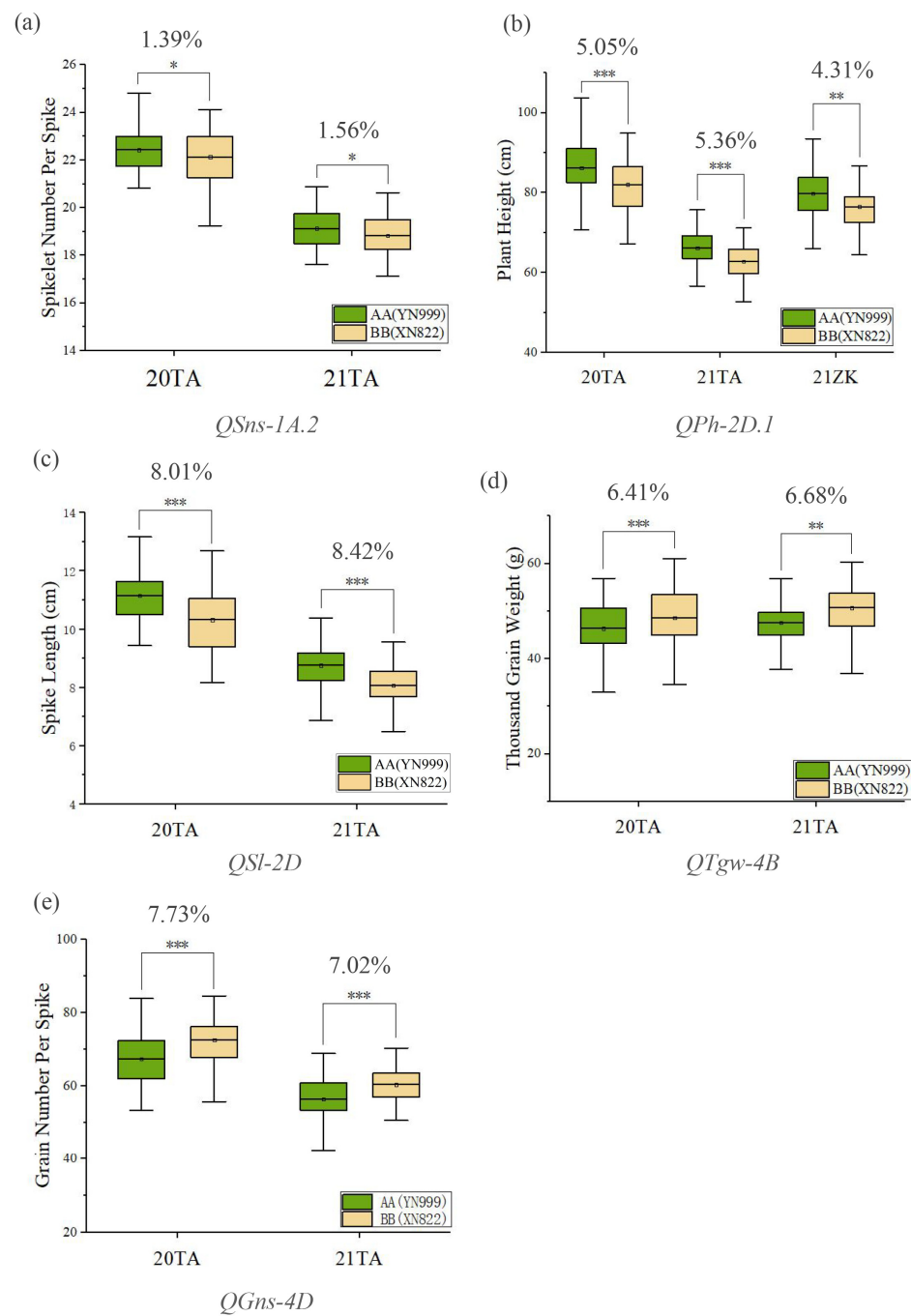


Figure 5. Effects of major QTLs *QSnS-1A.2* (a), *QPh-2D.1* (b), *QSl-2D* (c), *QTgw-4B* (d), and *QGns-4D* (e) on corresponding traits in the RILs population. XN822 and YN999 indicate the lines with the alleles from XN822 and YN999, respectively; *, ** and *** represent significance determined by the Student's *t* test at $p < 0.05$, $p < 0.01$ and $p < 0.001$, respectively; X-axis refers to environments and Y-axis refers to trait values. The green and yellow colors of boxplots refer to RILs carrying alleles from YN999 and XN822, respectively. The values above boxplots indicate average increased percentage between the two genotype groups.

QPh-2D.1 was detected in all of the experiments, and *QSl-2D* was detected in the 2020TA and 2021TA experiments with overlapped map locations of *QPh-2D.1* on 2D (Table 3). The RILs conferring the YN999 allele showed a 4.31% (2021ZK) to 5.36% (2021TA) increase in PH (Figure 5b), 8.01% (2020TA) and 8.42% (2021TA) increase in SL (Figure 5c) compared with those RILs with the XN822 allele for PH and SL.

QTgw-4B was detected in the 2020TA and 2021TA experiments; the allele from XN822 showed a positive effect on TGW. The RILs conferring the XN822 allele showed a 6.41% (2020TA) and 6.68% (2021TA) increase in TGW compared with those RILs with the YN999 allele (Figure 5d).

QGns-4D was detected in the 2020TA and 2021TA experiments; the allele from XN822 also showed a positive effect on GNS, with the RILs conferring the XN822 allele showing a 7.02% (2021TA) and 7.73% (2020TA) increase in GNS compared with those conferring the YN999 allele (Figure 5e).

4. Discussion

4.1. Consistent QTL with Previous Studies

Given the importance of wheat agronomic traits, a considerable amount of study has been undertaken to excavate genes controlling important agronomic traits [31–33]. In the present study, a total of 64 QTL related to agronomic traits were mapped, of which there were some QTL mapped to the same locations as in previous studies.

QPh-2D.1 could be repeatedly detected in all three experiments with the physical location of 21.61–32.34 Mb on 2D. *Rht8*, a major gene controlling PH, has been mapped to 24 Mb on 2D [34]. We inferred that *Rht8* may be the candidate gene for *QPh-2D.1*. In addition, *QPh-1A*, *QPh-3B.2*, and *QPh-7D.1* are consistent with the QTL discovered by Pang et al. (Table S1) [35].

QSl-6D and *QGl-6D* were mapped at the similar positions as QTL *QKL.caas-6DL* identified by Li et al. [18]. In addition, a stable QTL, *QSl-2D*, which was detected in two experiments in this study, was also reported by Li et al. (Table S1) [18].

QSns-2D.2 was mapped in the interval of 31.81–50.23 Mb on 2D in this study. Lin et al. [7] discovered a QTL associated with a grain number per spikelet between 28.09 and 34.43 Mb on 2D. We believe that a pleiotropic QTL for SNS and grain number per spikelet might be present here (Table S1).

The QTL *QGns-4A* and QTL *QGns-3B* had been reported in other studies [35,36]. The two QTL for SN *QSn-1B* and *QSn-6A* had also been reported in other studies [35,36]. Among the five QTL for TGW identified in this study, *QTgw-4A*, *QTgw-4B*, and *QTgw-7B* were consistent with QTL discovered by other studies [36–38] (Table S1).

QPh-4A was located between 616.67 Mb and 617.58 Mb on 4A (Table 3), which was close to *QPh.hvwgr-4AL* detected by Li et al. [39] and Gao et al. [36]. *QTgw-2A* was located between 603.5 Mb and 621.19 Mb on 2A, which was close to the QTL detected by Mérida-García et al. [38]. *QSns-2B* was located between 749.22 Mb and 756.00 Mb on 2B, which was close to *QSns.sau-AM-2B.2* detected by Mo et al. (Table S1) [40].

4.2. Novel QTL Mapped in this Study

Among the 12 QTL for PH, 7, including *QPh-2B*, *QPh-2D.2*, *QPh-3B.1*, *QPh-6B*, *QPh-6D*, *QPh-7A*, and *QPh-7D.2*, appeared to be novel QTL identified by this study. Among them, *QPh-7D.2* was detected in all the experiments and explained 9.18% to 10.76% of the phenotypic variation. Thus, developing molecular markers in this region will benefit the MAS of this QTL.

For spike traits, seven of the nine QTL for SL, including *QSl-2A*, *QSl-3D*, *QSl-4A*, *QSl-4B*, *QSl-5D*, *QSl-7B*, and *QSl-7D*, appeared to be novel QTL. Among them, *QSl-2A* was detected in all experiments and explained 3.03% to 10.98% of the phenotypic variation. Six of the eight QTL for SNS, including *QSns-1A.2*, *QSns-1A.1*, *QSns-1B*, *QSns-2D.1*, *QSns-6A.1*, and *QSns-6A.2*, appeared to be novel QTL. QTL *QSns-1A.2* could be detected as a stable QTL in both 2020TA and 2021TA experiments, and the SNS of the RILs conferring the allele from YN999 significantly increased the SNS by 1.39% and 1.56% in the 2020TA and 2021TA experiments, respectively (Figure 5a); therefore, we can further design molecular markers to fine-map and clone the gene. Four of the six QTL for GNS, including *QGns-2A.1*, *QGns-2A.2*, *QGns-4D*, and *QGns-6A*, appeared to be novel QTL. *QGns-4D* were detected in the 2020TA and 2021TA experiments, which explained 13.54% and 12.16% of the phenotypic

variation, respectively. The positive allele of this locus was contributed to by XN822. In the population, RILs conferring the XN822 allele showed a 7.02% (2021TA) and 7.73% (2020TA) increase in GNS compared with those conferring the YN999 allele (Figure 5e), indicating that this QTL is highly valuable in increasing SNS; thus, further fine-mapping and cloning of this QTL are highly valuable not only for the understanding of the molecular mechanism of this gene regulating the GNS, but also for the increase in GNS in breeding.

For grain traits, one QTL for TGW, *QTgw-1D*, appears to be a novel QTL. Six of the seven QTL for the GL, including *QGl-2A*, *QGl-4A.1*, *QGl-4A.2*, *QGl-6A*, *QGl-7A*, and *QGl-7B*, appeared to be novel QTL. Two QTL for the GW appeared to be novel QTL. All the QTL for Sur and Peri appeared to be novel QTL. We speculated that this may be due to the small number of studies of the two traits.

4.3. Beneficial Alleles from Both Parents

YN999 and XN822 contributed 33 and 31 beneficial positive QTL alleles for all QTL, respectively. YN999 contributed more positive alleles for SN (2), TGW (3), GL (4), Peri (6), and Sur (3), whereas XN822 contributed more positive alleles for PH (8), SL (6), SNS (6), GNS (4), and GW (2), indicating that both of them confer different favorable alleles for different traits. It is highly valuable to identify and pyramid these favorable alleles to develop new cultivars with improved agronomic traits and a higher yield.

In contrast to previous studies [7,21,31], the positive alleles of the identified QTL mainly originated from parents with relatively high phenotypic values, which is attributed to the significant phenotypic differences between the two parents, and the parent with relatively high phenotypic values containing more of the positive alleles. In this study, both parents are elite cultivars and exhibited superior phenotypes. XN822 showed 53.61 g of TGW, 6.32 mm of GL and 3.45 mm of GW in the 2021TA experiment with excellent grain traits. YN999 showed 11.16 cm of SL, 22.34 of SNS and 8.56 of SN in the 2020TA experiment with excellent spike traits. Given the excellent trait performance and the complementarity of the two parents in different traits, there is a high probability of mapping some agronomic trait-related QTL in this population. Therefore, we chose XN822 and YN999 as the parents to develop the RILs population, and both of them contributed beneficial QTL alleles for different traits. Thus, it is possible to pyramid these positive alleles to develop lines conferring positive alleles from both parents and the selection of such lines is currently underway.

4.4. Pleiotropic QTLs

The pleiotropy of a QTL refers to the phenomenon where a single QTL locus simultaneously influences two or more quantitative traits. Pleiotropic QTL reveal the relationship between complex traits. The marker-assisted selection of the mapped pleiotropic QTL can facilitate a genetic improvement for multiple related traits simultaneously. Many pleiotropic QTL have been discovered in wheat. For example, three pleiotropic QTL regions for total SNS and heading date were detected on chromosomes 2A, 7A, and 7D by Chen et al. [41]. Deng et al. [42] identified a QTL with pleiotropic effects for SN, SL, and GNS. Zhang et al. [43] discovered a QTL located on chromosome 7DL exhibiting pleiotropic effects for both leaf rust and powdery mildew resistance. The QTL located on 5DL could provide pleiotropic resistance against both leaf rust and stripe rust [43].

In the present study, seven pleiotropism QTL were identified on chromosomes 1A, 2A, 2D, 4A (2), 5B, and 6D for PH, SL, GL, Peri, and Sur. The PVE of each QTL was 3.91–38.24%. Developing molecular markers in these areas will benefit the MAS for multiple traits.

4.5. Use of the Developed KASP Assays

The KASP assay is a quick and cost-effective genotyping assay for single SNP analysis [44,45] that has been successfully applied in polyploids such as wheat [46]. Thus, it is a useful SNP genotyping platform for the MAS. In the present study, four most closely linked SNPs to five QTL (*QSns-1A.2*, *QPh-2D.1*, *QSl-2D*, *QTgw-4B*, and *QGns-4D*) were converted

into KASP markers and run across the RIL population. Comparison of the two contrasting genotypes at each locus further validated the effects of each QTL to the phenotype with those RILs carrying the positive allele at the five loci had significantly greater values of the corresponding traits than the RILs conferring the negative allele. Thus, these KASP markers are diagnostic for phenotypic changes and can be widely used for the MAS of these QTL in breeding.

5. Conclusions

In summary, 64 QTL for agronomically important traits were mapped, while 46 of them were putative novel QTL. Nine of the mapped QTL were detected in multiple experiments and explained a large percentage of phenotypic variations, which can be further fine-mapped and cloned. KASP assays closely linked with five major QTL were developed and validated, which can be widely used in the MAS and fine-mapping of these QTL. This study laid an important foundation for the discovery of genes underlying agronomically important traits in elite wheat cultivars and provided useful molecular markers for the MAS of agronomic important traits in breeding. Further MAS breeding using these KASPs are underway to develop high-yield elite breeding.

Supplementary Materials: The following supporting information can be downloaded at: <https://www.mdpi.com/article/10.3390/agronomy14050940/s1>, Table S1: Comparison of QTL mapped in this study with reported genes/QTL in other studies.

Author Contributions: S.L. conceived the research. J.L. and S.L. wrote the manuscript; J.L., D.W., M.L., M.J., X.S., Y.P., Q.Y. and C.L. performed experiments; J.L. and Y.P. analyzed the data. All authors have read and agreed to the published version of the manuscript.

Funding: This work was supported by the Shandong Province Agricultural Fine Seeds Project (grant number 2022LZGC001 and 2023LZGC009), the National Natural Science Foundation of China (grant number 32072052), and the Taishan Scholars Program.

Data Availability Statement: The data presented in this study are available on request from the corresponding author on reasonable request.

Conflicts of Interest: The authors declare no conflicts of interest.

References

1. Chen, Y.E.; Cui, J.M.; Su, Y.Q.; Zhang, C.M.; Ma, J.; Zhang, Z.W.; Yuan, M.; Liu, W.J.; Zhang, H.Y.; Yuan, S. Comparison of Phosphorylation and Assembly of Photosystem Complexes and Redox Homeostasis in Two Wheat Cultivars with Different Drought Resistance. *Sci. Rep.* **2017**, *7*, 12718. [[CrossRef](#)]
2. Mwadzingeni, L.; Shimelis, H.; Tesfay, S.; Tsilo, T.J. Screening of Bread Wheat Genotypes for Drought Tolerance Using Phenotypic and Proline Analyses. *Front Plant Sci.* **2016**, *25*, 1276. [[CrossRef](#)] [[PubMed](#)]
3. Hu, J.; Wang, X.; Zhang, G.; Jiang, P.; Chen, W.; Hao, Y.; Ma, X.; Xu, S.; Jia, J.; Kong, L.; et al. QTL Mapping for Yield-Related Traits in Wheat Based on Four RIL Populations. *Theor. Appl. Genet.* **2020**, *133*, 917–933. [[CrossRef](#)]
4. Kennedy, G.; Matsuzaki, H.; Dong, S.L.; Liu, W.M.; Huang, J.; Liu, G.Y.; Su, X.; Cao, M.Q.; Chen, W.W.; Zhang, J.; et al. Large-scale genotyping of complex DNA. *Nat Biotechnol.* **2003**, *21*, 1233–1237. [[CrossRef](#)]
5. Bonin, A.; Bellemain, E.; Bronken, E.P.; Pompanon, F.; Brochmann, C.; Taberlet, P. How to track and assess genotyping errors in population genetics studies. *Mol Ecol.* **2004**, *13*, 3261–3273. [[CrossRef](#)]
6. Anderson, E.C.; Garza, J.C. The power of single-nucleotide polymorphisms for large-scale parentage inference. *Genetics* **2006**, *172*, 2567–2582. [[CrossRef](#)] [[PubMed](#)]
7. Muhammad, A.; Hu, W.; Li, Z.; Li, J.; Xie, G.; Wang, J.; Wang, L. Appraising the Genetic Architecture of Kernel Traits in Hexaploid Wheat Using GWAS. *Int. J. Mol. Sci.* **2020**, *21*, 5649. [[CrossRef](#)]
8. Luo, Q.; Zheng, Q.; Hu, P.; Liu, L.; Yang, G.; Li, H.; Li, B.; Li, Z. Mapping QTL for Agronomic Traits under Two Levels of Salt Stress in a New Constructed RIL Wheat Population. *Theor. Appl. Genet.* **2020**, *134*, 171–189. [[CrossRef](#)]
9. Bennani, S.; Birouk, A.; Jlibene, M.; Sanchez-Garcia, M.; Nsarellah, N.; Gaboun, F.; Tadesse, W. Drought-Tolerance QTLs Associated with Grain Yield and Related Traits in Spring Bread Wheat. *Plants* **2022**, *11*, 986. [[CrossRef](#)]
10. Liu, J.; Luo, W.; Qin, N.; Ding, P.; Zhang, H.; Yang, C.; Mu, Y.; Tang, H.; Liu, Y.; Li, W.; et al. A 55 K SNP Array-Based Genetic Map and Its Utilization in QTL Mapping for Productive Tiller Number in Common Wheat. *Theor. Appl. Genet.* **2018**, *131*, 2439–2450. [[CrossRef](#)]

11. Huang, S.; Wu, J.; Wang, X.; Mu, J.; Xu, Z.; Zeng, Q.; Liu, S.; Wang, Q.; Kang, Z.; Han, D. Utilization of the Genomewide Wheat 55K SNP Array for Genetic Analysis of Stripe Rust Resistance in Common Wheat Line P9936. *Phytopathology* **2019**, *109*, 819–827. [[CrossRef](#)]
12. Ren, T.; Hu, Y.; Tang, Y.; Li, C.; Yan, B.; Ren, Z.; Tan, F.; Tang, Z.; Fu, S.; Li, Z. Utilization of a Wheat 55K SNP Array for Mapping of Major QTL for Temporal Expression of the Tiller Number. *Front. Plant Sci.* **2018**, *9*, 333.
13. Zhou, C.Y.; Xiong, H.C.; Li, Y.T.; Gou, H.J.; Xie, Y.D.; Zhao, L.S.; Gu, J.Y.; Zhao, S.R.; Ding, Y.P.; Song, X.Y.; et al. Genetic Analysis and QTL Mapping of a Novel Reduced Height Gene in Common Wheat (*Triticum aestivum* L.). *J. Integr. Agric.* **2020**, *19*, 1721–1730. [[CrossRef](#)]
14. Russo, M.A.; Ficco, D.B.M.; Laidò, G.; Marone, D.; Papa, R.; Blanco, A.; Gadaleta, A.; De Vita, P.; Mastrangelo, A.M. A Dense Durum Wheat × T. Dicotyledon Linkage Map Based on SNP Markers for the Study of Seed Morphology. *Mol. Breed.* **2014**, *34*, 1579–1597. [[CrossRef](#)]
15. Echeverry-Solarte, M.; Kumar, A.; Kianian, S.; Simsek, S.; Alamri, M.S.; Mantovani, E.E.; McClean, P.E.; Deckard, E.L.; Elias, E.; Schatz, B.; et al. New QTL Alleles for Quality-Related Traits in Spring Wheat Revealed by RIL Population Derived from Supernumerary × Non-Supernumerary Spikelet Genotypes. *Theor. Appl. Genet.* **2015**, *128*, 893–912. [[CrossRef](#)]
16. Zhang, K.; Wang, J.; Zhang, L.; Rong, C.; Zhao, F.; Peng, T.; Li, H.; Cheng, D.; Liu, X.; Qin, H.; et al. Association Analysis of Genomic Loci Important for Grain Weight Control in Elite Common Wheat Varieties Cultivated with Variable Water and Fertiliser Supply. *PLoS ONE*. **2013**, *8*, e57853. [[CrossRef](#)]
17. Liu, J.; Xu, Z.; Fan, X.; Zhou, Q.; Cao, J.; Wang, F.; Ji, G.; Yang, L.; Feng, B.; Wang, T. A Genome-Wide Association Study of Wheat Spike Related Traits in China. *Front. Plant Sci.* **2018**, *871*, 1584.
18. Li, F.; Wen, W.; He, Z.; Liu, J.; Jin, H.; Cao, S.; Geng, H.; Yan, J.; Zhang, P.; Wan, Y.; et al. Genome-Wide Linkage Mapping of Yield-Related Traits in Three Chinese Bread Wheat Populations Using High-Density SNP Markers. *Theor. Appl. Genet.* **2018**, *131*, 1903–1924. [[CrossRef](#)] [[PubMed](#)]
19. Wolde, G.M.; Trautewig, C.; Mascher, M.; Schnurbusch, T. Genetic Insights into Morphometric Inflorescence Traits of Wheat. *Theor. Appl. Genet.* **2019**, *132*, 1661–1676. [[CrossRef](#)]
20. Yao, H.; Xie, Q.; Xue, S.; Luo, J.; Lu, J.; Kong, Z.; Wang, Y.; Zhai, W.; Lu, N.; Wei, R.; et al. HL2 on Chromosome 7D of Wheat (*Triticum aestivum* L.) Regulates Both Head Length and Spikelet Number. *Theor. Appl. Genet.* **2019**, *132*, 1789–1797. [[CrossRef](#)]
21. Chai, L.; Chen, Z.; Bian, R.; Zhai, H.; Cheng, X.; Peng, H.; Yao, Y.; Hu, Z.; Xin, M.; Guo, W.; et al. Dissection of Two Quantitative Trait Loci with Pleiotropic Effects on Plant Height and Spike Length Linked in Coupling Phase on the Short Arm of Chromosome 2D of Common Wheat (*Triticum aestivum* L.). *Theor. Appl. Genet.* **2018**, *131*, 2621–2637. [[CrossRef](#)]
22. Chen, Z.; Cheng, X.; Chai, L.; Wang, Z.; Bian, R.; Li, J.; Zhao, A.; Xin, M.; Guo, W.; Hu, Z.; et al. Dissection of Genetic Factors Underlying Grain Size and Fine Mapping of QTgw.Cau-7D in Common Wheat (*Triticum aestivum* L.). *Theor. Appl. Genet.* **2020**, *133*, 149–162. [[CrossRef](#)]
23. Ma, J.; Zhang, H.; Li, S.; Zou, Y.; Li, T.; Liu, J.; Ding, P.; Mu, Y.; Tang, H.; Deng, M.; et al. Identification of Quantitative Trait Loci for Kernel Traits in a Wheat Cultivar Chuannong16. *BMC Genet.* **2019**, *20*, 77. [[CrossRef](#)]
24. Yang, L.; Zhao, D.; Meng, Z.; Xu, K.; Yan, J.; Xia, X.; Cao, S.; Tian, Y.; He, Z.; Zhang, Y. QTL Mapping for Grain Yield-Related Traits in Bread Wheat via SNP-Based Selective Genotyping. *Theor. Appl. Genet.* **2020**, *133*, 857–872. [[CrossRef](#)]
25. Xu, D.; Wen, W.; Fu, L.; Li, F.; Li, J.; Xie, L.; Xia, X.; Ni, Z.; He, Z.; Cao, S. Genetic Dissection of a Major QTL for Kernel Weight Spanning the Rht-B1 Locus in Bread Wheat. *Theor. Appl. Genet.* **2019**, *132*, 3191–3200. [[CrossRef](#)] [[PubMed](#)]
26. Sun, C.; Zhang, F.; Yan, X.; Zhang, X.; Dong, Z.; Cui, D.; Chen, F. Genome-Wide Association Study for 13 Agronomic Traits Reveals Distribution of Superior Alleles in Bread Wheat from the Yellow and Huai Valley of China. *Plant Biotechnol. J.* **2017**, *15*, 953–969. [[CrossRef](#)]
27. Xin, F.; Zhu, T.; Wei, S.; Han, Y.C.; Zhao, Y.; Zhang, D.Z.; Ma, L.J. QTL Mapping of Kernel Traits and Validation of a Major QTL for Kernel Length-Width Ratio Using SNP and Bulk Segregant Analysis in Wheat. *Sci. Rep.* **2020**, *10*, 25. [[CrossRef](#)]
28. Rasheed, A.; Xia, X.; Ogbonnaya, F.; Mahmood, T.; Zhang, Z.; Mujeeb-Kazi, A.; He, Z. Genome-Wide Association for Grain Morphology in Synthetic Hexaploid Wheats Using Digital Imaging Analysis. *BMC Plant Biol.* **2014**, *14*, 128. [[CrossRef](#)]
29. Winfield, M.O.; Allen, A.M.; Burrridge, A.J.; Barker, G.L.A.; Benbow, H.R.; Wilkinson, P.A.; Coghill, J.; Waterfall, C.; Davassi, A.; Scopes, G.; et al. High-Density SNP Genotyping Array for Hexaploid Wheat and Its Secondary and Tertiary Gene Pool. *Plant Biotechnol. J.* **2016**, *14*, 1195–1206. [[CrossRef](#)]
30. Bariana, H.; Forrest, K.; Qureshi, N.; Miah, H.; Hayden, M.; Bansal, U. Adult plant stripe rust resistance gene Yr71 maps close to Lr24 in chromosome 3D of common wheat. *Mol. Breeding.* **2016**, *36*, 98. [[CrossRef](#)]
31. Ding, P.Y.; Mo, Z.Q.; Tang, H.P.; Mu, Y.; Deng, M.; Jiang, Q.T.; Liu, Y.X.; Chen, G.D.; Chen, G.Y.; Wang, J.R.; et al. A Major and Stable QTL for Wheat Spikelet Number per Spike Validated in Different Genetic Backgrounds. *J. Integr. Agric.* **2022**, *21*, 1551–1562.
32. Heidari, B.; Sayed-Tabatabaei, B.E.; Saeidi, G.; Kearsley, M.; Suenaga, K. Mapping QTL for Grain Yield, Yield Components, and Spike Features in a Doubled Haploid Population of Bread Wheat. *Genome* **2011**, *54*, 517–527. [[CrossRef](#)]
33. Sidhu, G.; Mohan, A.; Zheng, P.; Dhaliwal, A.K.; Main, D.; Kulvinder, S. Sequencing-based high throughput mutation detection in bread wheat. *BMC Genom.* **2015**, *16*, 962. [[CrossRef](#)]
34. Xiong, H.; Zhou, C.; Fu, M.; Guo, H.; Xie, Y.; Zhao, L.; Gu, J.; Zhao, S.; Ding, Y.; Li, Y.; et al. Cloning and Functional Characterization of Rht8, a “Green Revolution” Replacement Gene in Wheat. *Mol. Plant.* **2022**, *15*, 373–376. [[CrossRef](#)] [[PubMed](#)]

35. Pang, Y.; Liu, C.; Wang, D.; St. Amand, P.; Bernardo, A.; Li, W.; He, F.; Li, L.; Wang, L.; Yuan, X.; et al. High-Resolution Genome-Wide Association Study Identifies Genomic Regions and Candidate Genes for Important Agronomic Traits in Wheat. *Mol. Plant*. **2020**, *13*, 1311–1327. [[CrossRef](#)]
36. Gao, F.; Wen, W.; Liu, J.; Rasheed, A.; Yin, G.; Xia, X.; Wu, X.; He, Z. Genome-Wide Linkage Mapping of QTL for Yield Components, Plant Height and Yield-Related Physiological Traits in the Chinese Wheat Cross Zhou 8425B/Chinese Spring. *Front. Plant Sci.* **2015**, *6*, 1099. [[CrossRef](#)]
37. Hu, W.; Gao, D.; Liao, S.; Cheng, S.; Jia, J.; Xu, W. Identification of a Pleiotropic QTL Cluster for Fusarium Head Blight Resistance, Spikelet Compactness, Grain Number per Spike and Thousand-Grain Weight in Common Wheat. *Crop J.* **2023**, *11*, 672–677. [[CrossRef](#)]
38. Mérida-García, R.; Bentley, A.R.; Gálvez, S.; Dorado, G.; Solís, I.; Ammar, K.; Hernandez, P. Mapping Agronomic and Quality Traits in Elite Durum Wheat Lines under Differing Water Regimes. *Agronomy* **2020**, *10*, 144. [[CrossRef](#)]
39. Li, C.; Bai, G.; Carver, B.F.; Chao, S.; Wang, Z. Mapping Quantitative Trait Loci for Plant Adaptation and Morphology Traits in Wheat Using Single Nucleotide Polymorphisms. *Euphytica* **2016**, *208*, 299–312. [[CrossRef](#)]
40. Mo, Z.; Zhu, J.; Wei, J.; Zhou, J.; Xu, Q.; Tang, H.; Mu, Y.; Deng, M.; Jiang, Q.; Liu, Y.; et al. The 55K SNP-Based Exploration of QTLs for Spikelet Number Per Spike in a Tetraploid Wheat (*Triticum turgidum* L.) Population: Chinese Landrace “Ailanmai” × Wild Emmer. *Front. Plant Sci.* **2021**, *12*, 732837. [[CrossRef](#)]
41. Chen, Z.; Cheng, X.; Chai, L.; Wang, Z.; Du, D.; Wang, Z.; Bian, R.; Zhao, A.; Xin, M.; Guo, W.; et al. Pleiotropic QTL Influencing Spikelet Number and Heading Date in Common Wheat (*Triticum aestivum* L.). *Theor. Appl. Genet.* **2020**, *133*, 1825–1838. [[CrossRef](#)] [[PubMed](#)]
42. Deng, S.; Wu, X.; Wu, Y.; Zhou, R.; Wang, H.; Jia, J.; Liu, S. Characterization and Precise Mapping of a QTL Increasing Spike Number with Pleiotropic Effects in Wheat. *Theor. Appl. Genet.* **2011**, *122*, 281–289. [[CrossRef](#)] [[PubMed](#)]
43. Zhang, P.; Lan, C.; Asad, M.A.; Gebrewahid, T.W.; Xia, X.; He, Z.; Li, Z.; Liu, D. QTL Mapping of Adult-Plant Resistance to Leaf Rust in the Chinese Landraces Pingyuan 50/Mingxian 169 Using the Wheat 55K SNP Array. *Mol. Breed.* **2019**, *39*, 98. [[CrossRef](#)]
44. Terracciano, I.; Maccaferri, M.; Bassi, F.; Mantovani, P.; Sanguineti, M.C.; Salvi, S.; Šimková, H.; Doležel, J.; Massi, A.; Ammar, K.; et al. Development of COS-SNP and HRM Markers for High-Throughput and Reliable Haplotype-Based Detection of Lr14a in Durum Wheat (*Triticum durum* Desf.). *Theor. Appl. Genet.* **2013**, *126*, 1077–1101. [[CrossRef](#)] [[PubMed](#)]
45. Semagn, K.; Babu, R.; Hearne, S.; Olsen, M. Single Nucleotide Polymorphism Genotyping Using Kompetitive Allele Specific PCR (KASP): Overview of the Technology and Its Application in Crop Improvement. *Mol. Breed.* **2014**, *33*, 1–14. [[CrossRef](#)]
46. Allen, A.M.; Barker, G.L.A.; Berry, S.T.; Coghill, J.A.; Gwilliam, R.; Kirby, S.; Robinson, P.; Brenchley, R.C.; D’Amore, R.; Mckenzie, N.; et al. Transcript-Specific, Single-Nucleotide Polymorphism Discovery and Linkage Analysis in Hexaploid Bread Wheat (*Triticum aestivum* L.). *Plant Biotechnol. J.* **2011**, *9*, 1086–1099. [[CrossRef](#)]

Disclaimer/Publisher’s Note: The statements, opinions and data contained in all publications are solely those of the individual author(s) and contributor(s) and not of MDPI and/or the editor(s). MDPI and/or the editor(s) disclaim responsibility for any injury to people or property resulting from any ideas, methods, instructions or products referred to in the content.